Diffuse interface modeling of a radial vapor bubble collapse

2015 J. Phys.: Conf. Ser. 656 012028

(http://iopscience.iop.org/1742-6596/656/1/012028)

Journal of Physics: Conference Series **656** (2015) 012028 doi:10.1088/1742-6596/656/1/012028

Diffuse interface modeling of a radial vapor bubble collapse

Francesco Magaletti, Luca Marino, Carlo Massimo Casciola

Dipartimento di Ingegneria Meccanica e Aerospaziale, Università di Roma "La Sapienza", via Eudossiana 18, 00184 Roma Italy

E-mail: `francesco.magaletti@uniroma1.it`

Abstract. A diffuse interface model is exploited to study in details the dynamics of a cavitation vapor bubble, by including phase change, transition to supercritical conditions, shock wave propagation and thermal conduction. The numerical experiments show that the actual dynamic is a sequence of collapses and rebounds demonstrating the importance of non-equilibrium phase changes. In particular the transition to supercritical conditions avoids the full condensation and leads to shockwave emission after the collapse and to successive bubble rebound.

1. Introduction

The collapse of a vapor bubble is a classical but still crucial phenomenon in the realm of the physics of fluids [1]. The interest is twofold, being aimed at the analysis and a better comprehension of the complex physical mechanisms involved in the processes and to the important possible applications which range from the cavitation over ship propellers to the drug delivery strategy in biological systems.

Collapse bubble dynamics is difficult to model since several spatial and time scales can be involved in the same process. Moreover non trivial effects like phase transition to and from supercritical conditions or shock formation can easily be encountered. As the bubble radius decreases the surface tension at the interface becomes more and more relevant and the condensation and compression phenomena can lead to extreme pressure and temperatures.

Experimental results are usually based on visual analysis carried out with high speed cameras which can give a quantitative description or indirect information [2]. On the other hand, numerical results can be particularly demanding and very sensitive to the mathematical model adopted. Recently more detailed physical models have been proposed to study the dynamics of the bubble interface [3, 4], possibly taking into account the presence of a dissolved gas [5].

We present the results obtained by a diffuse interface model based on the van der Waals free energy functional. Following this approach the effects of the capillarity are naturally embedded in the physical model and it is possible to deal with the interface dynamic as well as with complex phase change phenomena. The collapse of the vapor bubble has been thoroughly studied, in particular in the case where the interface speed may exceed the speed of sound. In this peculiar condition, the complex dynamic of shock waves, focused towards the bubble and successively reflected back in the liquid, has been analyzed and discussed. Furthermore we considered in

details the effects of condensation and of rapid compression which locally bring the vapor in supercritical conditions.

2. Mathematical model and numerical solution

Vapor bubble dynamics is a particular case of the most general two-phase interfacial flows phenomena. The fluid dynamic modeling of interfacial problems has been a challenge for theoreticians due to their intrinsic multi-scale nature. Indeed the interfacial (i.e. capillary) properties of a liquid-vapor system, acting on the molecular length scale, strongly interact with the characteristic macroscopic length scale of the fluid dynamic problem. In the last decades several different models have been proposed to describe liquid-vapor systems endowing capillary stresses and they can be grouped into the two main categories of sharp and diffuse interface approaches (see the review [6]).

In this work we adopt an unsteady diffuse interface model coupled with the choice of van der Waals state equation (see [7, 8] for details). This model can be deduced introducing a suitable non-local free energy functional $F[\rho,\theta]$ with a gradient type excess energy:

$$F[\rho,\theta]=\int_\Omega\left(\hat{f}_0\left(\rho,\theta\right)+\frac{\lambda}{2}|\boldsymbol{\nabla}\rho|^2\right)dV\,, \tag{1}$$

where λ is a coefficient strongly related to the interfacial properties of the liquid-vapor system (i.e. surface tension and interface thickness) and $\hat{f}_0\left(\rho,\theta\right)$ the bulk free energy density per unit volume of a uniform fluid at temperature θ and density ρ. In particular, we choose the van der Waals free energy for a polytropic fluid (constant volume specific heat c_v) whose expression follows:

$$\hat{f}_0\left(\rho,\theta\right)=\bar{R}\rho\theta\left[-1+\log\left(\frac{\rho\,K\,\theta^{1/\delta}}{1-b\rho}\right)\right]-a\rho^2\,, \tag{2}$$

with $\delta=\bar{R}/c_v$, $\bar{R}$ the gas constant, a and b the van der Waals gas constants and K a constant related to the de Broglie length [9].

Given the thermodynamic behavior of the inhomogeneous system, its fluid dynamics, under the assumption of spherical symmetry, is described by the following conservation laws for mass, momentum and total energy densities

$$\frac{\partial\rho}{\partial t}+\frac{1}{r^2}\frac{\partial}{\partial r}\left(r^2\rho u_r\right)=0\,, \tag{3}$$

$$\frac{\partial\rho u_r}{\partial t}+\frac{1}{r^2}\frac{\partial}{\partial r}\left(r^2\rho u_r^2\right)=-\frac{\partial p_0}{\partial r}+\frac{1}{r^2}\frac{\partial}{\partial r}\left(r^2T_{rr}\right)-\frac{2T_{\phi\phi}}{r}\,, \tag{4}$$

$$\frac{\partial E}{\partial t}+\frac{1}{r^2}\frac{\partial}{\partial r}\left[r^2u_r\left(E+p_0\right)\right]=\frac{1}{r^2}\frac{\partial}{\partial r}\left[r^2\left(T_{rr}u_r-\lambda\rho\frac{\partial\rho}{\partial r}\frac{1}{r^2}\frac{\partial}{\partial r}\left(r^2u_r\right)+k\frac{\partial\theta}{\partial r}\right)\right]\,, \tag{5}$$

with u_r the radial component of the fluid velocity and k the thermal conductivity. The stress tensor $\boldsymbol{T}$ in the equations takes into account both the viscous and diffused capillary stresses and its relevant components read:

$$T_{rr}=\lambda\left[-\frac{1}{2}\left(\frac{\partial\rho}{\partial r}\right)^2+\frac{\rho}{r^2}\frac{\partial}{\partial r}\left(r^2\frac{\partial\rho}{\partial r}\right)\right]+2\mu\left[\frac{\partial u_r}{\partial r}-\frac{1}{3r^2}\frac{\partial}{\partial r}\left(r^2u_r\right)\right]\,, \tag{6}$$

$$T_{\phi\phi}=\lambda\left[\frac{1}{2}\left(\frac{\partial\rho}{\partial r}\right)^2+\frac{\rho}{r^2}\frac{\partial}{\partial r}\left(r^2\frac{\partial\rho}{\partial r}\right)\right]+2\mu\left[\frac{u_r}{r}-\frac{1}{3r^2}\frac{\partial}{\partial r}\left(r^2u_r\right)\right]\,, \tag{7}$$

The classical thermodynamic pressure p_0 for a van der Waals fluid is readily obtained from Eq. (2):

$$p_0 = -\frac{\partial f_0}{\partial v} = -\frac{\partial \hat{f}_0/\rho}{\partial v} = \bar{R}\frac{\rho\theta}{1-b\rho} - a\rho^2\,, \tag{8}$$

with $f_0 = \hat{f}_0/\rho$ the specific bulk free energy and $v = 1/\rho$ the specific volume.

The system of equations in (3-5) is numerically challenging because it contains several phenomena, asking for specific numerical techniques. The first aspect is the presence of the moving and extremely thin liquid-vapor interface that requires a great amount of grid points in order to correctly capture the capillary stress. Another issue is related to the formation of shock waves, hence the numerical scheme needs to be based on shock-capturing method, such as ENO or WENO schemes [10]. These methods work only with hyperbolic equations, but the presence of viscosity and capillarity implies a non-hyperbolic nature of the equations. A classical Strang operator-splitting addresses this issue, isolating the viscous and capillary operators discretized with classical central finite difference from the hyperbolic part where a WENO scheme is used. The boundary conditions of fixed pressure and temperature, far away from the bubble, are imposed with a characteristic-wave approach [11]. Further details can be found in [8].

3. Results and discussion

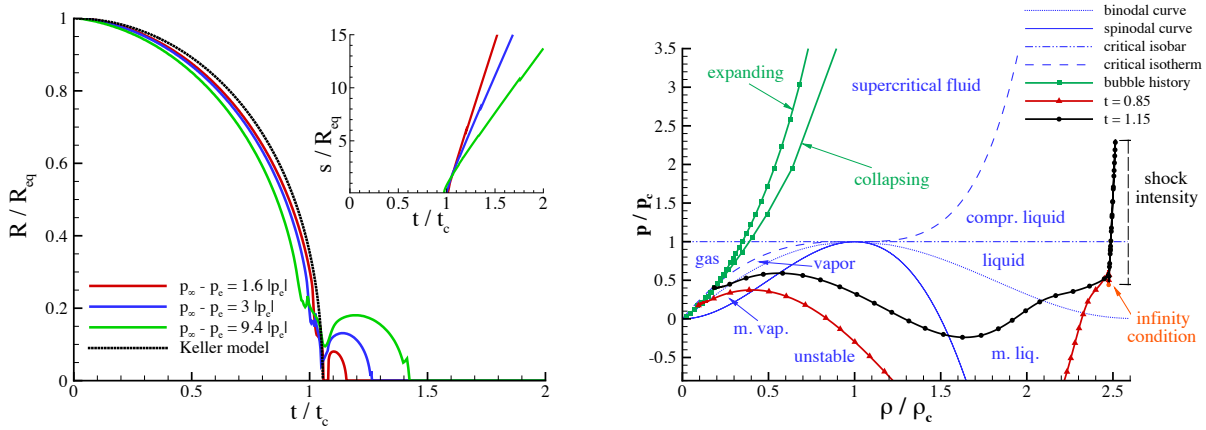

Figure 1. In the left panel, the radius evolution for different overpressure in the liquid. The inset shows the position of the shock radiated after the collapse with the same colors of the main plot. In the right panel, the evolution of the thermodynamic condition in the $p-\rho$ plane (with p_c and ρ_c the critical pressure and density, respectively). The green curve represents the conditions at the bubble center along the evolution. The red and black curves represent the conditions in the whole domain at two different time instant, before and after the collapse, respectively

The system is initially in equilibrium with a pure vapor bubble of radius R_{eq} immersed in its liquid at pressure p_e. The radial collapse is initiated by imposing an overpressure in the liquid $\Delta p = p_\infty - p_e$. Along the evolution the bubble radius is defined as the distance of the liquid from the bubble center, see the left panel of Fig. 1 where the radius evolution is plotted for different overpressures and is compared with the prediction of the Keller model [3]. The actual dynamic consists in a sequence of collapses and rebounds (that resembles the evolution of a pure gas bubble), while the simplified Keller model predicts a full condensation after the first collapse if no dissolved gas is added in the description. The key features that explains the rebounds is the transition of the vapor into supercritical state. The phase change into supercritical conditions, indeed, avoids the full condensation and allows the bubble rebound. When the bubble reaches

its minimum radius, a shockwave is radiated into the liquid phase, as shown in the inset of Fig. 1.

The thermodynamic conditions reached along the evolution are reported in the right panel of Fig.1. As background information (with blue lines), the figure provides the main thermodynamic features of the van der Waals system, e.g. critical isotherm and isobar, binodal and spinodal curve. The region between binodal and spinodal lines corresponds to metastable states (matestable liquid/vapor to the right/left of the critical density). In a finite size, equilibrium bubble, the vapor is in the corresponding metastable region, while the liquid state is inside the stable region to the right of the binodal line. The square symbols (green on line) show the thermodynamic state of the fluid occupying the bubble center at successive time instants during the first collapse/expansion phase. The evolution is towards increasing (decreasing) pressures during collapse (expansion). The two branches match at pressure higher than those reported in the diagram. During collapse, the fluid at the center of the bubble starts in the vapor region and follows the saturation line (binodal curve) only during the first stage of the collapse. Successively it enters the gas region to finally become supercritical reaching extremely high pressures and temperatures. The reverse sequence is observed during expansion. Triangles and circles (red and black lines, respectively) show the states of the fluid at changing radial position at two time instants, $t/t_c = 0.85$ during the collapse phase before the first rebound, and $t/t_c = 1.15$ during the successive expansion phase. In the latter curve, the steep pressure increase at high density (corresponding to liquid) is the pressure jump across the shockwave generated at rebound.

The transition to supercritical conditions is the key feature of the collapse of a vapor bubble. The rapid compression experienced by the vapor avoid the full condensation and leads to the transition to incondensable gaseous state. As a main consequence, the dynamic of a pure vapor bubble shows typical features of a pure gas bubble collapse such as shockwave emission and bubble rebounds, implying the importance of including phase change phenomena into the modeling of cavitation problems.

References

[1] Rayleigh L 1917 *The London, Edinburgh, and Dublin Philosophical Magazine and Journal of Science* **34** 94–98
[2] Taleyarkhan R P, West C, Cho J, Lahey R, Nigmatulin R and Block R 2002 *Science* **295** 1868–1873
[3] Keller J B and Kolodner I I 1956 *Journal of Applied Physics* **27** 1152–1161
[4] Plesset M S and Chapman R B 1971 *Journal of Fluid Mechanics* **47** 283–290
[5] Akhatov I, Lindau O, Topolnikov A, Mettin R, Vakhitova N and Lauterborn W 2001 *Physics of Fluids* **13** 2805–2819
[6] Anderson D, McFadden G and Wheeler A 1998 *Annual Review of Fluid Mechanics* **30** 139–165 ISSN 0066-4189
[7] Jamet D, Lebaigue O, Coutris N and Delhaye J 2001 *Journal of Computational Physics* **169** 624–651
[8] Magaletti F, Marino L and Casciola C 2015 *Physical Review Letters* **114** 064501
[9] Zhao N, Mentrelli A, Ruggeri T and Sugiyama M 2011 *Physics of Fluids* **23** 086101
[10] Shu C W 1998 *Essentially non-oscillatory and weighted essentially non-oscillatory schemes for hyperbolic conservation laws* (Springer)
[11] Poinsot T J and Lele S 1992 *Journal of computational physics* **101** 104–129